Preliminary Classification and Modeling of the Hysteretic Behavior of Connections in Timber Structures

Agnese Spedicato, Nicoló Vaiana, and Luciano Rosati

Abstract Timber connections are crucial to guarantee structural integrity and performance in timber structures, especially under cyclic loading scenarios such as those induced by earthquakes and winds. In addition, understanding the hysteretic behavior exhibited by these connections is essential to accurately predict their response. Researchers typically perform experimental tests to investigate the behavior of various types of connections; the latter typically exhibit different types of hysteresis loop shapes which, consequently, provide different values of stiffness, strength, and energy dissipation. This study aims to categorize and simulate such hysteresis loop shapes by using a recent phenomenological hysteresis model formulated by Vaiana and Rosati. The proposed approach also enables the deduction of crucial information, such as secant stiffness, equivalent damping ratio, and energy dissipation, which are relevant for simplifying the dynamic analysis of timber structures.

Keywords Hysteresis · Timber connections · Vaiana Rosati Model

1 Introduction

The structural performance of timber constructions under dynamic loading conditions, such as those imposed by seismic activity and strong winds, heavily depends on the integrity and behavior of their connections. Timber connections serve as critical junctions where loads are transferred between different structural elements, and their behavior under cyclic loading is essential for ensuring overall structural stability and safety.

Hysteresis is a phenomenon observed in many materials and structures subjected to cyclic loading, and it is described by a nonlinear relationship between the applied load and the resulting displacement, incorporating crucial information about stiffness, strength, and energy dissipation capacity. In timber connections, hysteretic behavior

A. Spedicato (✉) · N. Vaiana · L. Rosati
Department of Structures for Engineering and Architecture, University of Naples Federico II, via Claudio 21, 80125 Naples, Italy
e-mail: agnese.spedicato@unina.it

F. Marmo et al. (eds.), *Computational Mechanics and Applied Mathematics: Perspectives from Young Scholars*, Lecture Notes in Mechanical Engineering,
https://doi.org/10.1007/978-3-031-76591-9_10

is particularly significant due to the material's natural anisotropy and the complex interaction between the wood fibers and fasteners.

In scientific literature, numerous experimental investigations have been conducted to understand the behavior of various types of timber connections under cyclic loading. These studies reveal various hysteresis loop shapes, each corresponding to different mechanical properties and energy dissipation mechanisms. However, experimental approaches alone may not always be enough for comprehensive analysis and prediction due to their inherent time, cost, and feasibility limitations for large-scale structures.

To address these challenges, researchers have developed phenomenological hysteresis models that can simulate the observed behavior of timber connections with reasonable accuracy [1]. The model proposed by Vaiana and Rosati (VRM) [5–8, 10] stands out in this regard, offering a robust framework to categorize and replicate the hysteresis loop shapes observed in experimental tests. This model can take out essential parameters, such as secant stiffness, equivalent damping ratio, and dissipated energy, which are crucial for simplifying the dynamic analysis of timber structures. Using the VRM, this study contributes to a better understanding of the hysteretic behavior of timber structures related to the connection typology and the development of structures more capable of withstanding dynamic loads with greater efficiency.

2 Classification of Timber Connections

Understanding the various behaviors of timber connections under cyclic loading is fundamental for improving the strength of timber structures. Timber connections, critical in transferring loads between structural elements, exhibit various responses when subjected to dynamic forces such as earthquakes or strong winds. Classifying these connections based on their experimental hysteretic loop shapes provides valuable insights into their stiffness, strength, and energy dissipation capacities. In timber buildings, four categories of connections play a fundamental role:

1. *Angle Brackets*: these connections resist shear stress and are typically used to secure pillars or panels to the foundations or the floor. Their design is crucial for maintaining structural integrity under lateral loads.
2. *Hold-downs*: designed to resist tensile stress, hold-downs connect pillars or panels to foundations. They are essential in preventing uplift and ensuring that the structure remains anchored during dynamic loading events.
3. *Beam-to-Pillar connection*: designed in various ways, with or without intermediate plates. They play a key role in transferring loads between beams and pillars, influencing the overall stiffness and stability of the structure.
4. *Shear Wall connections*: used to connect two adjacent panels by screws, providing lateral stability to the structure. They are critical in resisting in-plane shear forces and contributing to the building's strength and stiffness.

The characteristic hysteretic behavior of these connections is more complex and varied compared to traditional materials like concrete or steel. As the loading and unloading phases take place, phenomena such as pinching and degradation often occur. Pinching refers to the reduction of the force in the central part of the hysteresis loop, generally due to the movement of metal fasteners within the timber. This movement creates frictional forces that alter stress and strain distribution. Degradation involves a reduction in strength and secant stiffness due to the loss of mechanical properties, typically occurring in the final phases of cyclic loading before failure.

Researchers often describe hysteresis behavior using the backbone curve (or skeleton/envelope curve), which captures variations in stiffness and strength over the loading history. This method allows for analyzing and comparing different designs, materials, and loading scenarios.

Another method for classifying hysteresis behavior involves using limiting curves, as proposed in [8], which categorize loop shapes into four types: (i) ***S1*** when delimited by two straight lines, (ii) ***S2*** when delimited by two curves without inflection points, (iii) ***S3*** when delimited by two curves with one inflection point, and (iv) ***S4*** when delimited by two curves with two inflection points.

Experimental tests from the scientific literature are studied and discussed to understand the general properties of the hysteretic behavior of timber connections.

Angle Bracket connection In a study examining the behavior of angle bracket connections, Gravic et al. [2] tested a specific connection type known as the Board Measured Foot (BMF) 90 × 116 × 48 × 3 mm, constructed using 11 annular ringed nails sized 4x60 mm, as depicted in Fig. 1a. The tests were performed on a Cross-Laminated Timber (CLT) panel consisting of five layers, each 17 mm thick, arranged orthogonally. The displacement velocity was between 0.4 and 0.8 mm/s during the cyclic testing. The connection demonstrated excellent performance, especially in shear, exhibiting significant ductility up to 30 mm displacement. The failure occurred when the steel nails yielded, forming two plastic hinges and causing slight ovalization of the holes around the nails. This study highlighted the connection's ability to withstand substantial deformations while maintaining its structural integrity, making it suitable for seismic applications. Considering the backbone curve in Fig. 1b, the connection strength increased with each cycle until reaching its peak resistance of approximately 27 kN at a deformation of 30 mm. After this point, the connection exhibited degradation in both strength and stiffness, ultimately leading to failure. From the point of view of limiting curves, the hysteresis loops became more complex throughout the test. The limiting curves began with an *S3* shape, with the inflection point shifting left to right during loading and right to left during unloading, eventually transitioning to an *S2* shape as the curves lost their inflection points.

Hold-down connection In the same scientific paper by Gravic et al. [2], researchers also investigated a hold-down connected to a CLT panel, which is 85 mm thick and consists of five orthogonally crossed layers. The hold-down used in the study was a WHT540 connected with 12 annular ringed nails Anker, each sized 4 × 60 mm. Both stationary and cyclic tests were conducted, with a velocity input ranging from 0.4 to 0.8 mm/s. The shear tests revealed significant connection deformation attributed to local steel buckling and nail withdrawal. Remarkably, the connection

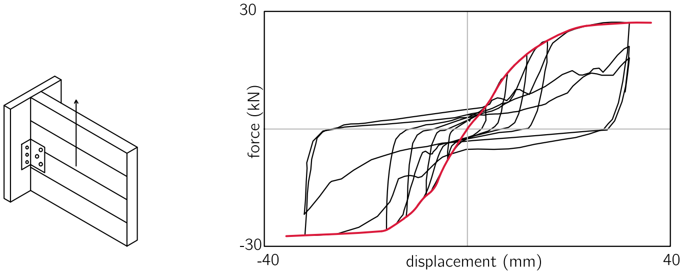

(a) (b)

Fig. 1 **a** Scheme of the specimen set-up of an angle bracket connected to a CLT panel loaded in shear tested in [2] and **b** hysteresis loop (black line) with associated backbone curve (red line)

exhibited a high level of displacement, approximately 47 mm, while exerting a limited force, around 15 kN, underscoring its capability to accommodate large displacements while retaining structural integrity. Examining the hysteretic response in Fig. 2, the backbone curve illustrates a gradual increase in connection strength during the cyclic test, accompanied by a slight reduction in secant stiffness in the latter part of the test. Furthermore, analysis of the limiting curves revealed a moderately pinched loop shape, indicative of enhanced energy dissipation capabilities compared to conventional timber connections. As the test progressed, further alterations in the limiting curves were observed, with the inflection point shifting from the left (right) side to the right (left) for the (un)loading curve. Finally, a reduction in the inner area of the loop occurred, with a strength and energy dissipation decay.

Beam-to-Pillar Connection The Master Thesis of Fairweather [3] provides insights into the behavior of beam-to-pillar connections. The specimen consisted

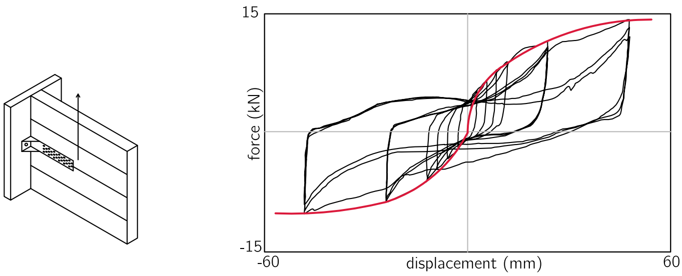

(a) (b)

Fig. 2 **a** Scheme of the specimen set-up of a hold-down connected to a CLT panel loaded in shear tested in [2] and **b** hysteresis loop (black line) with associated backbone curve (red line) of one continuous pillar and two beams connected to the pillar through steel brackets. Additionally, epoxy steel dowels were inserted at the ends of the beams and through the pillar. The glulam beams measured 495 × 135 mm, the glulam pillar was 495 × 180 mm, and the steel brackets were 500 × 150 mm. The test procedure involved quasi-static cyclic loading, with the lateral load increasing proportionally until the target was reached. The hysteresis loop in Fig. 3 exhibited a pinched shape but demonstrated a good capability to dissipate energy. The connection achieved a significant resistance of 50 kN with 50 mm of deformation, with slight strength degradation during the final cycles until failure occurred in the metal elements. Considering the limiting curves, the hysteresis loop shows a pinched nature with an *S3* shape characterized by one inflection point. During the trailing cycles, the limiting curves move to type *S2*, losing some internal area and energy dissipation capacity.

Shear Wall Connection In a study by Dong et al. [4], the behavior of single-shear nail connections in shear walls was tested. The specimens consisted of a 9.5 mm thick OSB panel connected with two 3.8 mm nails to a lumber element measuring 38 × 89 mm. Cyclic tests followed the CUREE loading protocol in ASTM-2126, characterized by increasing amplitudes and trailing secondary cycles. Figure 4 shows that from the beginning of the test, the hysteresis loop displayed intense pinching, with noticeable strength and secant stiffness degradation during the final cycles of the loading history. This behavior was particularly pronounced during the trailing cycles. Moreover, the limiting curves for the primary cycles were of type *S3*, with one inflection point that shifted during the loading history. The secondary cycles exhibited an *S2* shape with no inflection points, indicating the connection's reduced energy dissipation capacity as the test progressed.

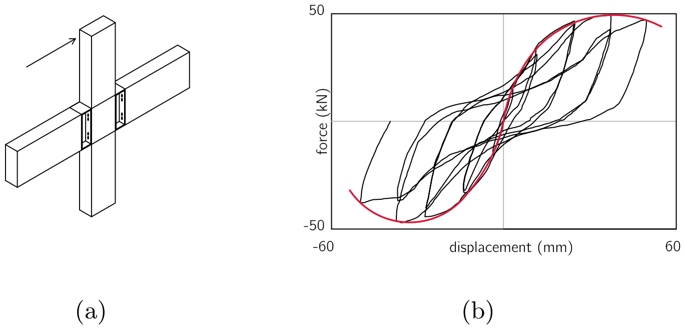

Fig. 3 **a** Scheme of the specimen set-up of beam-to-pillar connection loaded in shear tested in [3] and **b** hysteresis loop (black line) with associated backbone curve (red line)

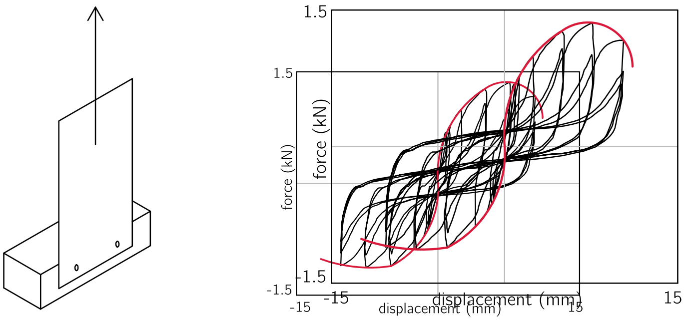

(a) (b)

Fig. 4 **a** Scheme of the specimen set-up of single shear wall connection tested in [4] and **b** hysteretic loop shape with specific backbone curve

3 The Vaiana-Rosati Model (VRM)

To simulate the complex hysteresis loops shown by timber connections, an accurate and very flexible hysteresis model is required. The Vaiana-Rosati Model (VRM) is a novel phenomenological hysteresis model formulated in [8–10], which gives several advantages when compared to existing hysteresis models. First, it evaluates the generalized hysteresis force, tangent stiffness, and work using closed-form equations. Additionally, the model is characterized by two independent sets of parameters, allowing for the simulation of asymmetric loop shapes and the pinching phenomenon. Furthermore, the parameters have clear physical and/or geometrical significance, making easier the parameters' calibration and reducing the need for manual effort. Finally, its mathematical formulation is user-friendly for computer software, making it suitable for widespread use in engineering applications.

The VRM is formulated in two different versions: analytical and differential. In this study, we use the analytical version (VRM+A) [10], which is briefly summarized in this section. In such a model, a generic hysteresis loop is described using two curves, the upper (c_u) and lower (c_l) curves, which are the asymptotes of the generic loading and unloading curves, respectively. The generalized force f_{ri} is a function of the generalized displacement u and the current point P, with its coordinates (u_P, f_P). If s is the sign of the generalized velocity $\dot{u}$, when $s > 0$ ($s < 0$), the set of model parameters is $k_b = k_b^+(k_b^-)$, $f_0 = f_0^+(f_0^-)$, $\alpha = \alpha^+(\alpha^-)$, $\beta_1 = \beta_1^+(\beta_1^-)$, $\beta_2 = \beta_2^+(\beta_2^-)$, $\gamma_1 = \gamma_1^+(\gamma_1^-)$, $\gamma_2 = \gamma_2^+(\gamma_2^-)$, $\gamma_3 = \gamma_3^+(\gamma_3^-)$.

Considering the generic time $t > t_P$, the generalized hysteretic force f_{ri} is evaluated as follows:

$$\begin{aligned} f_{ri}(t) = & f_e(t) + k_b u(t) + s(t) f_0 - [f_e(u(t_P)) + k_b u(t_P) \\ & + s(t) f_0 - f_{ri}(t_P)] e^{-s(t)\alpha(u(t)-u(t_P))}, \end{aligned} \quad (1)$$

Table 1 Initial set of VRM parameters adopted for simulating the experimental hysteresis loops shown in Figs. 5

Figure	s	k_b	f_0	α	β_1	β_2	γ_1	γ_2	γ_3
5a	+	0.18	11	1.1	−0.2	0.03	4.1	0.6	6.2
	−	0.2	12	1.0	−0.2	0.03	4.8	0.7	−6.2
5b	+	0.25	4.5	3.5	0.01	0.01	0.4	1.0	2.5
	−	0.1	1.7	1.6	0.01	0.01	0.6	1.0	−2.5
5c	+	0.1	21	0.5	0.0	0.0	10	0.2	5.0
	−	0.6	10	0.25	0.0	0.0	5.0	0.4	−7.0
5d	+	−0.001	0.5	5.0	0.4	0.1	0.2	3.0	0.8
	−	−0.001	0.5	5.0	0.4	0.1	0.2	2.5	−1.0

with:

$$f_e(t) = \beta_1 e^{\beta_2 u(t)} - \beta_1 + \frac{4\gamma_1}{1 + e^{-\gamma_2(u(t)-\gamma_3)}} - 2\gamma_1. \tag{2}$$

For brevity, the generalized tangent stiffness and work expressions are omitted and can be found directly in the paper [10].

4 Simulation of Experimental Hysteresis Loops

The experimental tests presented in Sect. 2 show the various hysteresis loop shapes of different timber connections, essential for comprehending their mechanical response to cyclic loading. The VRM is utilized to reproduce the experimental loop shapes, providing insights about connections, such as the energy dissipated during a dynamic event.

With reference to the experimental loops in Figs. 1, 2, 3, and 4, the calibration method begins by identifying the main phenomena affecting the loops during the loading history. Specifically, they are (i) the pinched loop shape, (ii) the shifting of the inflection point of the limiting curves, and (iii) the variation of the slope and strength degradation. These phenomena are simulated by adjusting specific model parameters. For instance, the parameter f_0 manages variations in amplitude during the loading cycle, while changes in the slope of the limiting curves are controlled by parameters β_1 and β_2. In addition, if the loop has a pinched shape, the parameters involved are γ_1, γ_2, γ_3, and in particular, if the inflection point moves from cycle to cycle, it is necessary to modify the parameter γ_3.

The second step of the calibration consists of the manual variation of the model parameters starting with a single cycle. The model parameters listed in Table 1 are obtained by imposing a sinusoidal displacement with increasing amplitude, and they allow for the simulation of the first cycle of each experimental loop shown in Fig. 5. Finally, by linking the variation of the model parameters to the dissipated energy, it

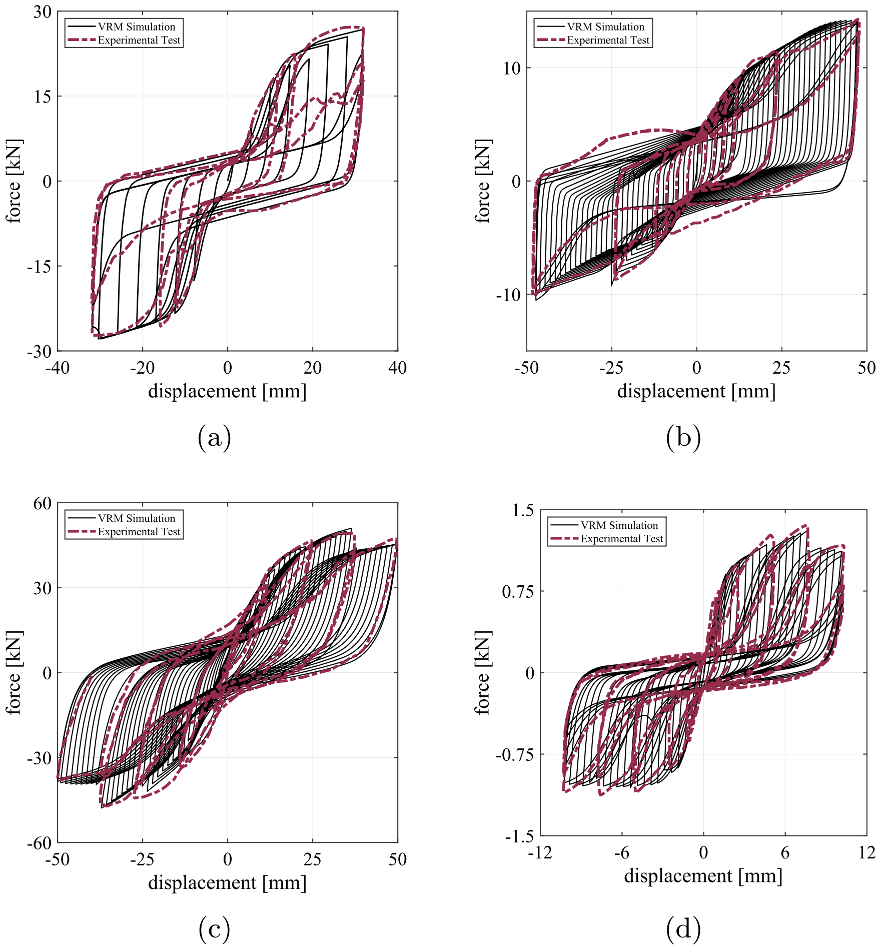

Fig. 5 Simulation of the experimental hysteresis loops using the VRM: **a** angle bracket and **b** hold-down tested by Gavric et al. [2], **c** beam-to-pillar connection tested by Fairweather [3] and **d** single shear wall tested by Dong et al. [4]

is possible to manipulate the shape of each single cycle, simulating the strength and secant stiffness degradation. Comparing the first and last sets of model parameters (Table 2), the values in bold represent the parameters that have been varied during the response to simulate the shape change.

The numerical simulation of the experimental hysteresis loops permits extracting fundamental information on the timber connections, such as the dissipated energy represented by the area enclosed by each hysteresis loop. We normalize the dissipated energy by using a reference energy value to facilitate comparison across different tests. This reference is obtained by multiplying the maximum hysteretic force by the

Table 2 Final set of VRM parameters adopted for simulating the experimental hysteresis loops shown in Fig. 5 changed as a function of the generalized work

Figure	s	k_b	f_0	α	β_1	β_2	γ_1	γ_2	γ_3
5a	+	0.18	11	1.1	−0.2	0.03	4.1	0.6	**31.03**
	−	0.2	12	1.0	−0.2	0.03	**3.56**	0.7	**−31.03**
5b	+	**0.52**	**7.80**	3.5	**1.06**	0.01	**2.25**	**0.14**	**42.08**
	−	**0.008**	**6.32**	**0.55**	**1.06**	0.01	**2.18**	**0.21**	**−42.08**
5c	+	**0.25**	**23.08**	**0.25**	0.0	0.0	**4.89**	0.2	**27**
	−	**0.23**	**16.22**	0.25	0.0	0.0	5.0	**0.2**	**−24.85**
5d	+	−0.001	0.5	**1.35**	**0.5**	**0.02**	0.2	**0.92**	**10.86**
	−	**0.0015**	0.5	**1.29**	**0.5**	**0.02**	0.2	**0.99**	**−11.06**

corresponding maximum displacement for each connection. The normalized dissipated energy is then computed as the ratio of the dissipated energy to the reference value, allowing for the comparison of the energy dissipation capacity of different timber connections on a common scale, thereby enabling an objective assessment of their performance under the same test conditions. Indeed, looking at Fig. 6, the Angle Bracket can dissipate more energy than the others, confirming its fundamental role in reacting to shear stress, such as in the case of horizontal actions.

5 Conclusions

The structural integrity and performance of timber connections under dynamic loading conditions are critical for ensuring timber constructions' overall safety and resilience. This study explored the hysteretic behavior of various timber connections under cyclic loading, providing insights into their stiffness, strength, and energy

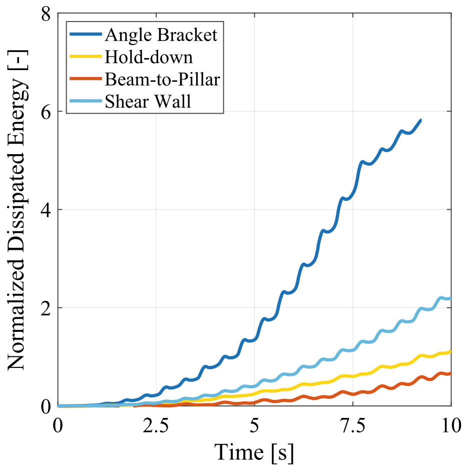

Fig. 6 Normalized energies dissipated by timber connections during the numerical simulations performed by imposing a sinusoidal displacement with increasing amplitude

dissipation capacities. Our classification and analysis of different types of timber connections – such as angle brackets, hold-downs, beam-to-pillar connections, and shear wall connections – demonstrate the variety of hysteresis loop shapes these connections exhibit. The pinching and strength degradation effects were particularly notable, highlighting the challenges and complexities inherent in the dynamic behavior of timber connections.

The VRM provides a robust framework for simulating and replicating the complex hysteresis loops observed by carefully calibrating the model parameters to match the experimental data. In addition, the study compared the dissipation capacity under similar loading conditions by quantifying the energy dissipated by the analyzed timber connections. These observations will be used in future work to numerically simulate the dynamic behavior of timber frames when different types of connections are installed in the same panel and to investigate their complex nonlinear dynamics [11, 12]. Starting from this study, we will also use the equivalent viscous damping approach to simplify the analysis and making easier to model and predict the behavior of timber frames under various loading scenarios.

References

1. Capuano R, Vaiana N, Pellecchia D, Rosati L (2022) A solution algorithm for a modified Bouc-Wen model capable of simulating cyclic softening and pinching phenomena. IFAC-PapersOnLine 55(20):319–324. https://doi.org/10.1016/j.ifacol.2022.09.115
2. Gravic I, Ceccotti A, Fragiacomo M (2011) Experimental cyclic tests on cross-laminated timber panels and typical connections, na
3. Fairweather RH (1992) Beam column connections for multi-storey timber buildings. Master's Thesis, University of Canterbury
4. Dong H, He M, Wang X, Christopoulos C, Li Z, Shu Z (2021) Development of a uniaxial hysteretic model for dowel-type timber joints in OpenSees. Construct Build Mater 288:123112. https://doi.org/10.1016/j.conbuildmat.2021.123112
5. Vaiana N, Sessa S, Marmo F, Rosati L (2018) A class of uniaxial phenomenological models for simulating hysteretic phenomena in rate-independent mechanical systems and materials. Nonlinear Dyn 93:1647–1669. https://doi.org/10.1007/s11071-018-4282-2
6. Vaiana N, Sessa S, Marmo F, Rosati L (2019) Nonlinear dynamic analysis of hysteretic mechanical systems by combining a novel rate-independent model and an explicit time integration method. Nonlinear Dyn 98:2879–2901. https://doi.org/10.1007/s11071-019-05022-5
7. Vaiana N, Sessa S, Rosati L (2021) A generalized class of uniaxial rate-independent models for simulating asymmetric mechanical hysteresis phenomena. Mech Syst Signal Process 146:106984. https://doi.org/10.1016/j.ymssp.2020.106984
8. Vaiana N, Rosati L (2023) Classification and unified phenomenological modeling of complex uniaxial rate-independent hysteretic responses. Mech Syst Signal Process 182:109539. https://doi.org/10.1016/j.ymssp.2022.109539
9. Vaiana N, Capuano R, Rosati L.: Evaluation of path-dependent work and internal energy change for hysteretic mechanical systems. Mech Syst Signal Process 186:109862. https://doi.org/10.1016/j.ymssp.2022.109862
10. Vaiana N, Rosati L (2023) Analytical and differential reformulations of the Vaiana-Rosati model for complex rate-independent mechanical hysteresis phenomena. Mech Syst Signal Process 199:110448. https://doi.org/10.1016/j.ymssp.2023.110448

11. Formica G, Vaiana N, Rosati L, Lacarbonara W (2021) Pathfollowing of high-dimensional hysteretic systems under periodic forcing. Nonlinear Dyn 103(4):3515–3528. https://doi.org/10.1007/s11071-021-06374-7
12. Capuano R, Vaiana N, Rosati L (2024) Frequency-response curves for rate-independent hysteretic mechanical responses of complex shape. Nonlinear Dyn 112(7):5151–5175. https://doi.org/10.1007/s11071-023-09273-1